Precision measurement of the decay rate of the negative positronium ion Ps^-

Hubert Ceeh, Christoph Hugenschmidt,* and Klaus Schreckenbach
Technische Universität München, Lehrstuhl E21, James-Franck-Straße 1, D-85747 Garching, Germany

Stefan A. Gärtner and Peter G. Thirolf
Ludwig-Maximilians-Universität München, Am Coulombwall 1, D-85748 Garching, Germany

Svenja M. Fleischer† and Dirk Schwalm‡
Max-Planck-Institut für Kernphysik, Saupfercheckweg 1, D-69117 Heidelberg, Germany
(Received 17 October 2011; published 13 December 2011)

The negative positronium ion Ps^- is a bound system consisting of two electrons and a positron. Its three constituents are pointlike leptonic particles of equal mass, which are subject only to the electroweak and gravitational force. Hence, Ps^- is an ideal object in which to study the quantum mechanics of a three-body system. The ground state of Ps^- is stable against dissociation but unstable against annihilation into photons. We report here on a precise measurement of the Ps^- ground-state decay rate Γ, which was carried out at the high-intensity NEutron induced POsitron source MUniCh (NEPOMUC) at the research reactor FRM II in Garching. A value of $\Gamma = 2.0875(50)\,\mathrm{ns}^{-1}$ was obtained, which is three times more precise than previous experiments and in agreement with most recent theoretical predictions. The achieved experimental precision is at the level of the leading corrections in the theoretical predictions.

DOI: 10.1103/PhysRevA.84.062508 PACS number(s): 36.10.Dr, 78.70.Bj

I. INTRODUCTION

The prediction of a bound state of two electrons and a positron, the negative positronium ion Ps^-, dates back to 1946 [1]. Since then, this elusive ion has been the subject of numerous theoretical investigations because it is a unique model system for studying three-body quantum mechanics. As its three constituents are of equal mass, the Born-Oppenheimer approximation cannot be applied [2], in contrast to other three-body systems like He^+ or H^-. Therefore, special techniques had to be developed to solve the full quantum mechanical three-body problem [3]. Many properties of the Ps^- ion including the decay rate [4,5], binding energy [6–12], and photodetachment cross sections [13,14] have been calculated using numerical approaches like the variational principle of Ritz or the correlation function hyperspherical harmonics method [6,15–17].

Only a few experimental studies have dealt so far with Ps^-. It actually took until 1981 before the first experimental proof of its existence was presented by Mills [18], followed by the first measurement of the Ps^- decay rate, which resulted in $\Gamma = 2.09\ \mathrm{ns}^{-1}$ with an accuracy of 4.3% [19]. Twenty years later, a new attempt was made in Heidelberg [20] to improve the experimental precision of the decay-rate measurement. Using a combination of the beam-foil technique, already used by Mills to produce Ps^-, together with an improved Ps^- detection method based on a stripping process, a decay rate of $\Gamma = 2.089(15)\ \mathrm{ns}^{-1}$, which was six times more precise, could be obtained [21,22]. Very recently, Michishio *et al.* [23] reported the first successful measurement concerning the photodetachment of Ps^-.

The present paper deals with an improved measurement of the decay rate of Ps^-. Due to the low intensity of the positron source used in the Heidelberg measurement, the derived decay rate was mainly limited by statistics. The experiment was therefore moved to the NEutron induced POsitron source MUniCh (NEPOMUC) facility at the FRM II research reactor in Garching, one of the most intense positron sources presently available [24]. The flux of positrons delivered by the remoderation stage of NEPOMUC was more than two orders of magnitude larger and allowed for a number of systematic studies, which led to several improvements of the experimental setup and to considerably better control of systematic uncertainties. Together with increased statistics, the accuracy of the Ps^- decay rate could be improved by a factor of three, resulting in

$$\Gamma = 2.0875(50)\,\mathrm{ns}^{-1}.$$

The achieved precision is on the order of the $O(\alpha)$ corrections to the decay rate.

II. THE PS^- DECAY RATE

As depicted schematically in Fig. 1, the two electrons in the ground state of Ps^- are in a relative singlet state, and as this is a spherical symmetric configuration there is no preferred orientation of the positron spin. The positron therefore may form either a singlet (triplet) state with one of the electrons and annihilate like para- (ortho-)positronium into an even (odd) number of photons. Even more, also the one photon decay is possible in this case as the second electron can compensate the photon recoil. The total decay rate of Ps^- is thus given by the sum over all partial decay rates $\Gamma_{n\gamma}$:

$$\Gamma = \sum_{n\geqslant 1} \Gamma_{n\gamma}. \quad (1)$$

*Present address: Forschungs-Neutronenquelle Heinz Maier-Leibnitz (FRM II), Lichtenbergstr. 1, D-85747 Garching, Germany.
†Present address: University of Washington, 180 NPL Bldg, Seattle, WA 98195, USA.
‡Present address: Weizmann Institute of Science, Revohot 76100, Israel.

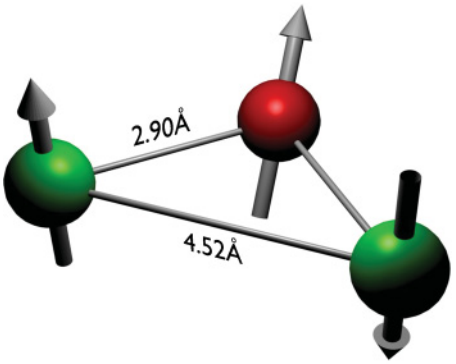

FIG. 1. (Color online) Artist's view of the Ps^- ion. The two electrons (green) are in a singlet state with their spins aligned antiparallel, while the spin orientation of the positron (red) is random. Averaged distances between the constituents are taken from [11].

In leading order in the fine structure constant α, the partial decay rates are found to be [25]

$$\begin{aligned}\Gamma^{(0)}_{2\gamma} &= \Gamma_0, \quad \Gamma^{(0)}_{3\gamma} = 0.123\alpha\Gamma_0,\\ \Gamma^{(0)}_{4\gamma} &= 0.0278\alpha^2\Gamma_0, \quad \Gamma^{(0)}_{5\gamma} = 0.00221\alpha^3\Gamma_0,\end{aligned} \tag{2}$$

with

$$\Gamma_0 = 2\pi\alpha^4 c a_0^{-1}\langle\delta_{+-}\rangle = 2.09280\,\mathrm{ns}^{-1}, \tag{3}$$

where c is the speed of light, a_0 is the Bohr radius, and α is the fine structure constant, while $\langle\delta_{+-}\rangle$ denotes the probability for finding an electron and the positron at the same position. The 1γ decay rate is given in leading order by

$$\Gamma^{(0)}_{1\gamma} = \frac{64\pi^2}{27}\alpha^8 c a_0^{-1}\langle\delta_{+--}\rangle = 3.82340\times10^{-2}\,\mathrm{s}^{-1} \tag{4}$$

with $\langle\delta_{+--}\rangle$ denoting the probability of finding all three particles at the same position [26]. Both $\langle\delta_{+-}\rangle$ and $\langle\delta_{+--}\rangle$ can be calculated from the Ps^- wave function obtained by a numerical solution of the three-body Schrödinger equation. The most recent values given in Refs. [5,11] were used to evaluate Eqs. (3) and (4).

It follows from Eqs. (2)–(4) that the total decay rate of Ps^- is dominated by the 2γ decay and that in first order in α the Ps^- decay rate is given by

$$\Gamma^{(0)} = \Gamma_0. \tag{5}$$

To account for the contribution of the $n\gamma$ decays with $n \geqslant 3$ as well as for other higher order QED terms and relativistic effects not considered by using the Schrödinger equation to calculate the ground-state wave function of Ps^-, it is convenient to expand Γ_{Ps^-} into a power series in α. As discussed in Ref. [5], one gets

$$\Gamma = \Gamma_0\left[1+\alpha A+\alpha^2\left(2\ln\frac{1}{\alpha}+B\right)+O(\alpha^3)\right]. \tag{6}$$

The first-order correction A has been well known for some time. It contains two contributions,

$$A = A^{2\gamma} + A^{3\gamma}, \tag{7}$$

with

$$A^{2\gamma} = \frac{\pi}{4} - \frac{5}{\pi} \tag{8}$$

being due to radiative corrections of $O(\alpha)$ to the 2γ decay and

$$A^{3\gamma} = \Gamma^{(0)}_{3\gamma}/\alpha\Gamma_0 = \frac{4\pi}{3} - \frac{12}{\pi} \tag{9}$$

being the leading-order contribution of the 3γ decay. The second-order contributions to Γ, which include the zero-order 4γ decay, corrections of $O(\alpha)$ to the 3γ, and corrections of $O(\alpha^2)$ to the 2γ decay, have recently been investigated by Puchalski *et al.* [5]. Including all contributions up to $O(\alpha^2)$, they calculated the total Ps^- decay rate to be

$$\Gamma = 2.087\,963(12)\ \mathrm{ns}^{-1}, \tag{10}$$

where the 6 ppm error is the estimated uncertainty due to the not-yet-calculated $O(\alpha^3)$ contributions.

The Ps^- ion is often regarded as a positronium atom with a loosely bound electron (see Fig. 1), which slightly changes the distance between the electron and positron but otherwise plays the role of a spectator. Indeed, taking into account the spin statistics and the different values for $\langle\delta_{+-}\rangle$, it is only the $O(\alpha^2)$ correction to the 2γ decay which contains corrections to the three-body wave function which are not contained in $\langle\delta_{+-}\rangle$ [5]. One should thus be able to estimate the Ps^- decay rate from the decay rates of ortho- and para-positronium by averaging over the initial spin states, that is,

$$\Gamma \approx \left(\tfrac{1}{4}\Gamma_{\mathrm{Para-Ps}} + \tfrac{3}{4}\Gamma_{\mathrm{Ortho-Ps}}\right), \tag{11}$$

and replacing $\langle\delta_{+-}\rangle = (16\pi)^{-1}$ (relevant for positronium) by the larger value of $\langle\delta_{+-}\rangle$ calculated for Ps^- [5]. Using the theoretical decay rates for ortho- and para-positronium [27], Eq. (11) results in

$$\Gamma \approx 2.0871\ \mathrm{ns}^{-1}, \tag{12}$$

which is indeed very close (within 4×10^{-4}) to the theoretical Ps^- decay rate given in Eq. (10).

III. EXPERIMENTAL SETUP

A. General description

In principle, the experiment follows the method applied in the previous experiment [22]: Ps^- ions are produced by letting positrons pass through a thin foil. The ions are accelerated to kilo-electron-volt energies, and the number of Ps^- ions surviving the passage through a gap of adjustable width is determined by stripping the ions and detecting the remaining positrons. The decrease of the number of surviving Ps^- with increasing gap width is directly reflecting the decay rate Γ_{Ps^-}.

A schematic view of the final experimental setup used in the decay-rate measurement at the NEPOMUC positron source

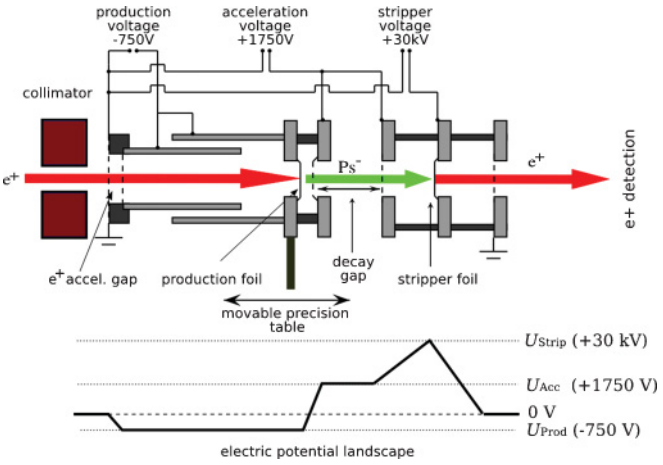

FIG. 2. (Color online) Schematic view of the experimental setup. From left to right: The positron postacceleration stage, the Ps^- production foil together with the Ps^- acceleration gap, which are mounted on a high-precision piezoelectric translation stage, the field-free decay gap, and the Ps^- stripping device. The positron detection unit attached to the stripping stage is shown separately in Fig. 3. The setup is immersed in a coaxial magnetic field of ≈60 Gauss, which is produced by several Helmholtz coils surrounding the vacuum chamber (not shown). Bottom part: The electric potential along the symmetry axis of the setup.

at the FRM II research reactor in Garching [24] is shown in Figs. 2 and 3. It is the result of several improvements to the original Heidelberg setup [21,22], which concern all three major components of the experiment: the postacceleration of the positrons towards the Ps^- production foil, the decay gap, which is now field free, and the positron detection after the stripping stage.

The primary 1-keV beam of moderated positrons provided by NEPOMUC ($9.0(8) \times 10^8$ e^+/s [28]) is first remoderated before being guided to the Ps^- setup in a solenoidal magnetic field. The remoderation stage [29], which has an efficiency of ≈5%, provides a positron beam of variable energy and a diameter of ≈2 mm (FWHM). For the present investigations, the positron energy was chosen to be $E_0 = 30$ eV.

The e^+ beam enters the experimental chamber through an aluminum collimator of 50 mm length and with a central bore of 5 mm in diameter. The positrons are then accelerated between two parallel grids and magnetically guided towards the Ps^- production foil. The magnetic guiding field is produced

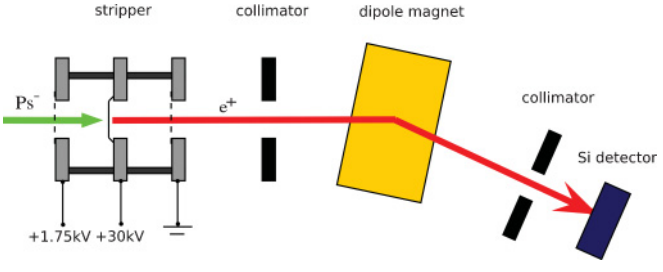

FIG. 3. (Color online) Schematic view of the positron detection stage. Positrons, leaving the stripping unit with a kinetic energy of ≈40 keV, are deflected by 15° using a dipole magnet and detected in a Si-surface barrier detector.

by several Helmholtz-like coils mounted outside the vacuum chamber, which produce a magnetic field of ≈60 Gauss in the axial direction with inhomogeneities along the spectrometer axis of less than 5%/10 cm. The accelerated positrons are shielded by two sliding tubes against electric stray fields mainly caused by the leads supplying the voltages to the various electrodes.

To produce Ps^- ions, diamondlike carbon (DLC) foils [30] are used, which have a diameter of 12 mm and thicknesses of around 5 nm. They are supported by a fine meshed copper grid (75-μm pitch) with an optical transmittance of 86%. These foils are known to be almost pin hole free (<1% [31]). Moreover, the foil used in the production run was checked before and after the measurements using a light microscope; no holes could be spotted. Positron slowing down in the foil and diffusing out of the surface have a certain chance to pick up two electrons and to form Ps^-. The acceleration voltage U_{Prod} of the positrons was chosen such that the observed rate of positronium ions was optimal. This required production voltages around $U_{\text{Prod}} = -750$ V.

A bismuth germanate (BGO) scintillation detector mounted outside of the vacuum chamber is used to monitor the incident positron flux. The detector is collimated such as to detect the e^+ annihilation occurring in the production foil. The intensity of the remoderated positron beam at the position of the production foil was estimated to be ≈1–2 × 10^7 e^+/s, which is a factor of 100 larger than in the precursor experiment [22].

The Ps^- ions, which are created at the surface of the DLC foil, are then accelerated to an energy of $(U_{\text{Acc}} - U_{\text{Prod}})e$ by a grid, which is mounted 2 mm behind the production foil and biased by U_{Acc}. The acceleration grid is a duplicate of the supporting grid of the DLC foil. After the acceleration, the Ps^- enter a field-free decay gap, the length d of which can be varied by a high-precision piezoelectric linear translation table from $d = 0.1$ mm up to $d = 40$ mm. The diameter of the Ps^- beam was found to be <4 mm (90% intensity), which is considerably smaller than the diameter of the entrance grid (12 mm) into the stripper stage (see also the discussion in Sec. III C).

The Ps^- ions surviving the drift through the decay gap are further accelerated in a tandem-like setup onto the stripper foil, a DLC foil similar to the production foil biased to +30 kV. By passing through the foil, the two electrons are stripped off the Ps^- ion and the remaining positron is further accelerated towards a grounded grid, thereby acquiring a total energy of ≈40 keV. This energetic positron, which is a unique signal that a Ps^- ion was formed in the production foil and survived the passage through the decay gap, is then observed with the help of a Si surface barrier detector.

A chicane made out of two Pb collimators and a dipole magnet, which deflects the positrons by 15°, is placed between the stripper and the positron detector (see Fig. 3). The chicane was introduced for efficient background suppression, as there is no direct line of sight from the detector to the production target, and secondary electrons produced by interactions of the copious annihilation quanta with the vacuum chamber walls are deflected opposite to the positrons. The Si detector has an active area of 300 mm^2 and is cooled to −20 °C to reduce the thermal noise; its nominal energy resolution for leptons is expected to be 12 keV. A 20-μm mylar foil is mounted in

front of the detector to stop positively charged ions, while the 40-keV positrons lose only ≈2 keV.

B. Control of the e^+ beam

Three ways to change the width d of the decay gap have been considered: (i) moving the e^+-acceleration stage together with the production foil, (ii) moving only the production foil, or (iii) moving only the stripper unit. It was finally decided that possible systematic errors could be best controlled by using the second procedure, which was therefore realized in the final setup (see Fig. 2).

The main challenge here is to avoid shifts of the accelerated e^+ beam on the production foil while the decay gap width is changed. As the Gaussian-shaped beam with its FWHM of ≈2 mm fits very well onto the area of the production foil (12 mm in diameter), and as any change of the direction of the impinging positrons is smeared out while traversing the foil, the main concerns are possible inhomogeneities or small pin holes of the DLC foil which might lead to a position-dependent Ps^- production probability. Great care was therefore taken to align all grids and foils to be parallel to each other and perpendicular to the central axis of the setup. The magnetic guiding field was adjusted to be parallel to the setup axis, and the drift gap of the accelerated positrons was shielded against stray electric fields. Moreover, the long Al-collimator ensured that the e^+ beam entered the setup on axis.

Several measurements were performed to test the quality of these measures. In one of them, the production foil was replaced by a grid followed by a microsphere plate to look for any lateral displacement of the beam as the precision table was moved. Within the precision of the measurement, no displacement of the beam was observed over the full range of 40 mm of the linear positioning unit. As the final decay rate measurement made use of a range of only 20 mm, the lateral shifts can be estimated to be less than 0.2 mm, which are small compared to the FWHM of the Gaussian e^+ beam.

The positron beam intensity was monitored by the BGO-scintillation detector, which detected the 511-keV annihilation quanta produced in the production foil, where the majority of the positrons annihilate. Since the detector was collimated to the zero position of the production foil, each gap width leads to a characteristic change of the count rate relative to the zero position. The long-term observation of the positron flux during the production run revealed that the positron intensity decreased approximately linearly with time at a rate of 7‰ per day. This decrease is attributed to a loss of efficiency of the remoderation stage caused by surface covering of the remoderation crystal with residual gas molecules. The decrease implies that during an average measurement cycle of 2.5 h, in which data were taken at each of the seven gap widths, the e^+ flux changed by about 1‰. By choosing a random order of the different gap widths during a cycle and collecting data over many cycles, these flux changes are averaged out. The BGO monitor was also used to identify short-term changes in the positron flux caused by (rare) perturbations through neighboring experiments or stray magnetic fields, for example from the movement of the crane in the experimental hall. If such a short-term variation occurred, the individual data set was excluded from the analysis.

C. The field-free decay gap

In the precursor experiment [22], the acceleration of the Ps^- ions and the decay gap were not separated; that is, the decay gap was also used to accelerate the Ps^- ions (in the following referred to as the Heidelberg method). While this looks like an elegant method to spare an additional grid, it could be a potential source of systematic errors. As the production voltage is adjusted such as to optimize the Ps^- production rate, which corresponds to e^+ energies where approximately half of the positrons are transmitted through the foil [20], due to scattering processes in the DLC foil some of the positrons leaving the foil will still have a sizable energy and may have acquired a large scattering angle. These positrons are reflected in the Ps^- acceleration field; most of them will return to the foil, where they might contribute to the Ps^- production rate, but others might miss it. As the strength of the Ps^- acceleration field depends on the acceleration voltage and on the width of the gap, such a scenario might lead to an acceleration voltage and gap-width-dependent Ps^- production rate.

The effect was actually discovered when several Ps^- decay-rate measurements were performed using the Heidelberg method at production voltages above the nominal value at which the Ps^- production probability is maximal. In Fig. 4, the relative Ps^- production rates and the deduced Ps^- decay rates Γ are shown as a function of the e^+ energy, which is given by $E_{e^+} = |U_{\mathrm{Prod}}|e + E_0$ with $E_0 = 30$ eV being the energy of the positron beam delivered from the remoderator; the Ps^- acceleration voltage, determined by $U_{\mathrm{Ps}^-} = U_{\mathrm{Acc}} - U_{\mathrm{Prod}}$, was kept constant at $U_{\mathrm{Ps}^-} = 3900$ V. The Ps^- decay rates [Fig. 4(b)], which were deduced from the decay curves following the procedure discussed in Ref. [22], are in agreement with the expected decay rate for positron energies $E_{e^+} \lesssim 700$ eV, where the production rate for this

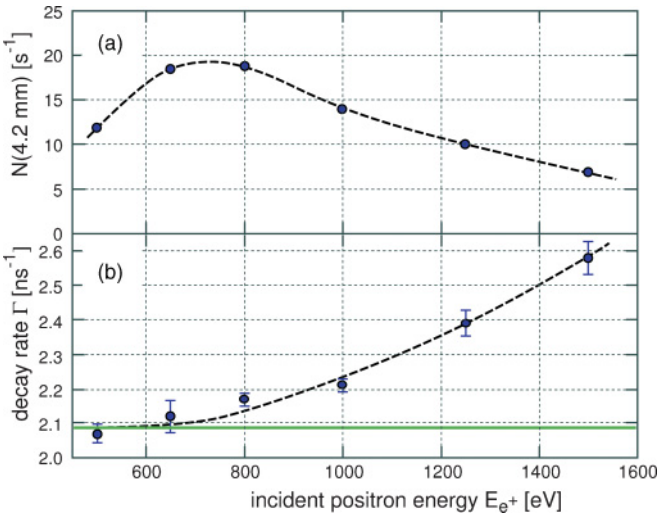

FIG. 4. (Color online) (a) Observed rate of Ps^- ions surviving a decay gap of 4.1 mm (statistical errors are of the size of the dots), and (b) Ps^- decay rates Γ, measured for different positron energies E_{e^+}. The measurements were performed using the Heidelberg method where the Ps^- ions are accelerated over the decay gap. The Ps^- acceleration voltage $U_{\mathrm{Ps}^-} = U_{\mathrm{Acc}} - U_{\mathrm{Prod}}$ was kept fixed at 3900 V. The solid (green) line is the expected decay rate; the dashed lines are to guide the eye.

particular DLC foil reaches its maximum [Fig. 4(a)]. At higher positron energies, however, the deduced decay rates deviate increasingly from the expected value.

As the size of the effect is rather astonishing, Monte Carlo simulations have been performed [32] in an attempt to understand these deviations at least qualitatively. Using reasonable assumptions about the energy and directional distributions of the positrons passing through the DLC foil, these studies show indeed that an increasing number of the reflected positrons may miss the production foil when the gap width is increased and may thus no longer contribute to the Ps^- production rate. As the sensitivity to this effect is expected to increase with decreasing acceleration voltages U_{Ps^-}, it might even be responsible for the small but consistently larger decay rates observed by Ref. [22] at acceleration voltages around 1000 V.

The effect can be easily avoided by separating the acceleration of the Ps^- ions from the decay gap. An additional grid similar to the supporting grid of the production foil was therefore mounted 2 mm behind the DLC foil and connected to the acceleration voltage U_{Acc}, while keeping the entrance grid to the stripper at the same potential (see Fig. 2). A field-free decay gap is created in this way. As the acceleration gap now stays constant, the Ps^- production rate can no longer be influenced by changing the decay gap, and the observed Ps^- decay rate Γ is independent of the energy of the positrons impinging on the DLC foil [33].

In the field-free decay gap, the Ps^- ions are drifting with a constant velocity $v = \beta c$. The number $N(d)$ of Ps^- surviving the drift distance d is thus given by

$$N(d) = N_0 \exp(-\mu d), \tag{13}$$

where the decay constant μ is connected to the decay rate Γ by

$$\Gamma = \mu \beta \gamma c. \tag{14}$$

The product of the velocity factor β and the Lorentz factor γ is found to be

$$\beta\gamma = \sqrt{\left(\frac{eU_{Ps^-} + T_0}{3m_e c^2} + 1\right)^2 - 1}, \tag{15}$$

with m_e being the mass of the electron. T_0 denotes the average kinetic energy of the nascent Ps^-, which is expected to be smaller than the binding energy of the second electron of 0.33 eV [8], an expectation in accordance with experimental findings [21]. We therefore assume T_0 to be $T_0 = 0.3 \pm 0.3$ eV.

D. The dipole chicane

The background seen by the Si detector could be reduced and flattened by inserting a magnetic dipole chicane between the stripper and the detector. A soft iron yoke with a gap width of 7 cm is used to produce a vertical magnetic field, which deflects the 40-keV positrons from the spectrometer axis towards the Si detector (see Fig. 3). The angle between the spectrometer axis and the detector axis can be varied between 0° and 25°. The spectral transmittance was tested with a ^{133}Ba source as a function of the magnetic field and the deflection angle. A deflection by 15° was found to be optimal. Compared to a measurement at 0° the signal-to-background ratio could be increased by a factor of 2, while the detection efficiency decreased only slightly by approximately 10%.

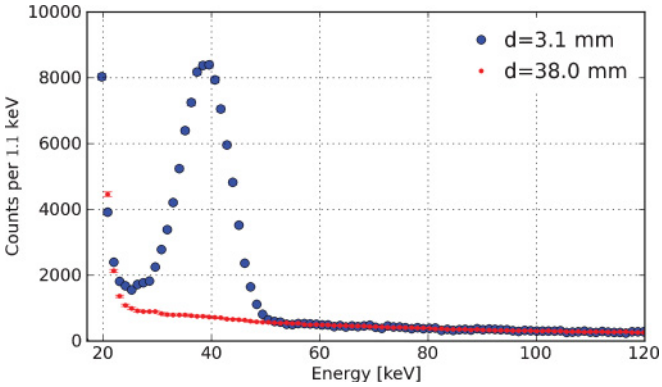

FIG. 5. (Color online) Energy spectra observed with the Si detector at decay gap widths of $d = 3.1$ mm and $d = 38$ mm, corresponding to 0.4 and 4.7 decay lengths, respectively. The energies of the positrons are shifted slightly below 40 keV due to the energy loss in the mylar foil mounted in front of the Si detector. The $d = 38$ mm spectrum was normalized to the one measured at $d = 3.1$ mm at energies above 55 keV.

Two energy spectra observed with the Si detector using the setup and voltage settings as shown in Figs. 2 and 3 are displayed in Fig. 5. In the spectrum recorded at a gap width of $d = 3.1$ mm, the peak resulting from the detection of the 40-keV positrons is clearly resolved from the electronic noise, which starts to dominate the spectrum below 25 keV. The measured resolution of the positron peak is 11.7 keV, even slightly below the nominal energy resolution of the Si detector of 12 keV. Due to the limited range of the precision table, the largest decay gap that can be reached is $d = 38$ mm, which is thus the closest we can get to a pure background spectrum. Although there is still a small contribution of 40-keV positrons present, the spectrum shows that the background above 25 keV is flat and structureless. The procedure adopted to derive a pure background spectrum is discussed in the following section.

IV. ANALYSIS AND RESULTS

In a production run involving 10 days of data taking, the number of surviving Ps^- ions was measured at seven decay gaps of $d = 3.1, 6.1, 8.1, 12.1, 16.1, 21.1$, and 38.0 mm. The measurement was divided in cycles of 3 h, in which all distances were measured in a random order. The measuring time for each distance was chosen—with the exception of the "background" spectrum at 38.0 mm—such as to reach a comparable number of Ps^- counts at all distances. The production voltage U_{Prod} was set to -750 V, and the Ps^- acceleration voltage $U_{Ps^-} = U_{Acc} - U_{Prod}$ was measured to be 2498 ± 1 V. The summed-up spectra recorded at each gap distance are plotted in Fig. 6.

An iterative method, similar to the one used previously [21], was applied to decompose the spectrum into the signal and a background contribution. In the first iteration step, it is assumed that the spectrum observed at $d = 38$ mm contains no Ps^- contribution. By normalizing this spectrum to the background region of the spectra measured at smaller gap widths, a background-corrected Ps^- count rate can be deduced and a first guess of the decay constant μ_1 is obtained. In

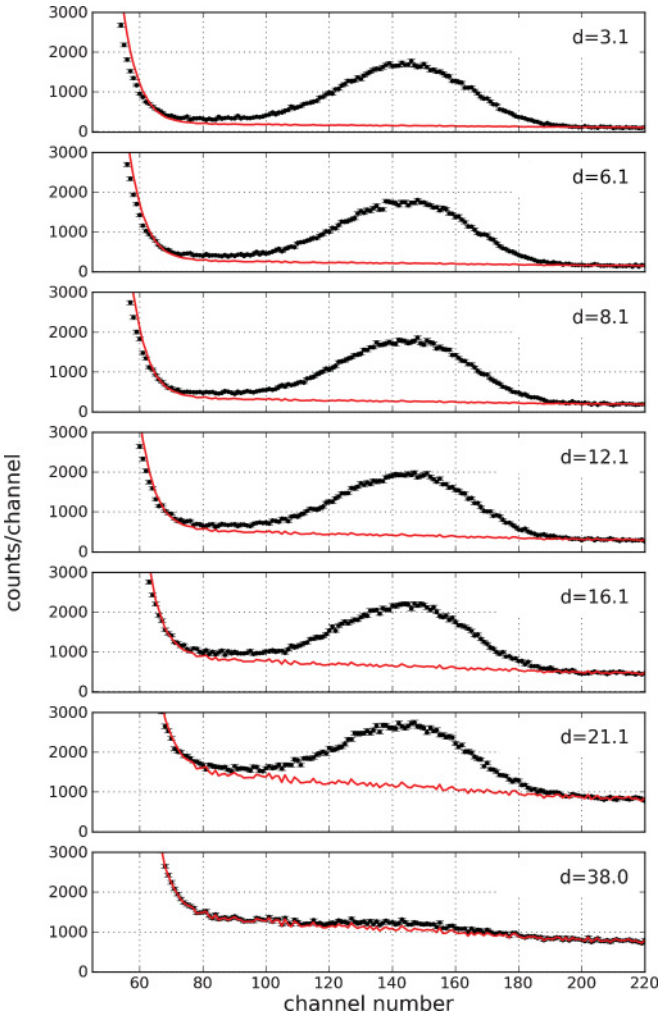

FIG. 6. (Color online) Positron spectra observed at seven decay-gap widths after summing over all measurement cycles (black dots). The solid (red) line represents the background spectrum derived from the measurement at $d = 38$ mm as discussed in the main text.

the second step, this decay constant is used to calculate the expected Ps^- count rate in the 38-mm spectrum, and the background-corrected Ps^- spectrum obtained at $d = 3.1$ mm is normalized accordingly and subtracted from the measured 38-mm spectrum to obtain a new guess for the background. This procedure is repeated until the value for the decay constant μ converges. The final background spectrum resulting from this iterative procedure is given by the solid (red) line in Fig. 6. The Ps^- spectra obtained after subtracting the background spectrum are displayed in Fig. 7.

The sensitivity of the deduced decay constant μ against changes of the integration limits used in the background normalization and against changes of the limits used for integrating the Ps^- peak was carefully investigated. For all reasonable variations, the observed differences are well within the statistical uncertainty of μ. The same is found to be true when deducing the Ps^- count rates by fitting the original spectra with an experimental Ps^- line shape, obtained by summing up the individual spectra shown in Fig. 7, and the final background spectrum. The Ps^- count rates derived in this way are displayed in Fig. 8 together with the best exponential

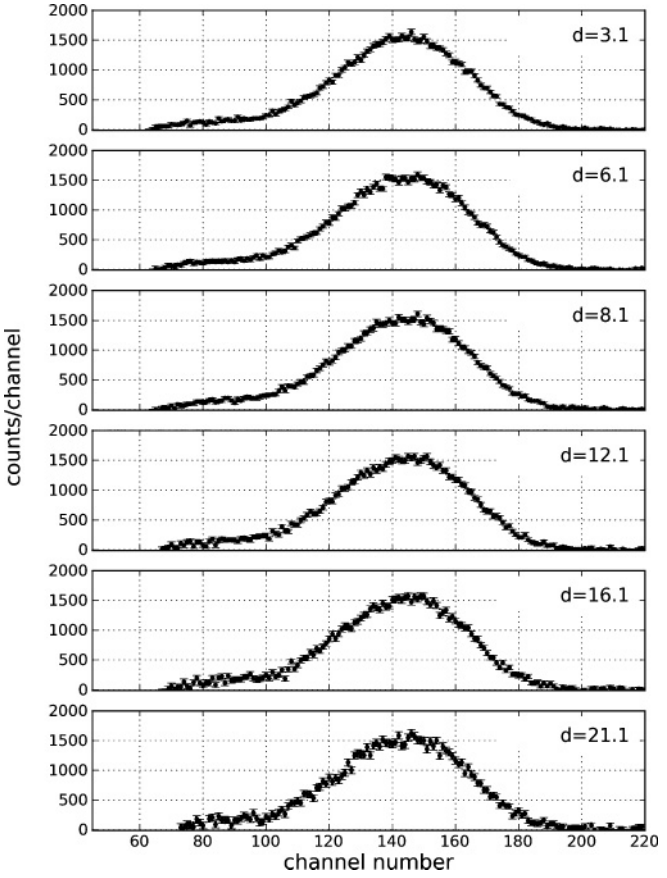

FIG. 7. Background-corrected positron spectra.

fit obtained from a χ^2-fitting procedure. The fit results in

$$\mu = (0.121\,94 \pm 0.000\,26)\,\mathrm{mm}^{-1}, \tag{16}$$

where the error given is the statistical error estimated with the MINOS routine of the MINUIT numerical minimization

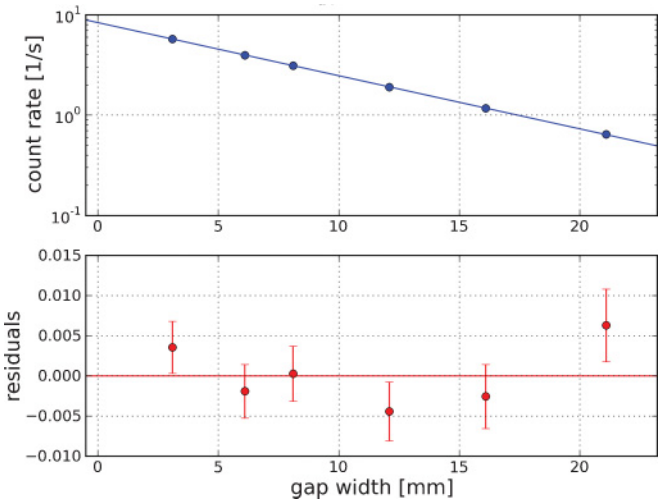

FIG. 8. (Color online) Top: Decay curve for Ps^- at an acceleration voltage of 2498 V. The statistical error bars of the individual Ps^- count rates are smaller than the symbols. The solid line represents the best fit by an exponential decay law. Bottom: Residuals observed with respect to the best fit.

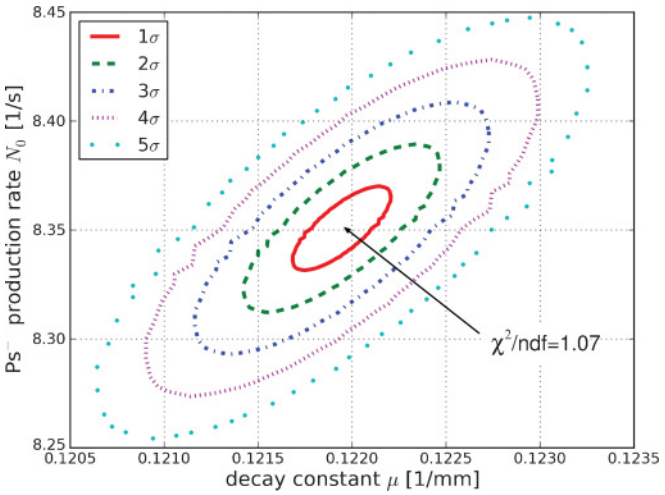

FIG. 9. (Color online) Contour plot of confidence levels in the space spanned by the two fitting parameters N_0 and μ from the χ^2 fitting of the decay curve by $N(d) = N_0 \exp(-\mu d)$.

package [34] (see Fig. 9). Using Eqs. (14) and (15), this result can be readily converted to a Ps^- decay rate of $\Gamma = (2.0875 \pm 0.0044)\,ns^{-1}$.

Several sources of possible systematic errors that could influence the Ps^- decay rate measurement have to be considered. They include the accuracy with which the Ps^- energy in the field-free decay gap is known, the sensitivity of the Ps^- production rate on the position of the e^+ beam on the DLC foil, the stability of the positron flux, the positioning accuracy of the linear translation table, and the timing accuracy of the data acquisition system.

The accuracy of the Ps^- energy is determined by the absolute value and the stability of the acceleration voltage $U_{Ps^-} = (U_{Accel} - U_{Prod})$ and by the initial Ps^- energy T_0. The acceleration voltage was continuously monitored by a high-precision voltmeter with an absolute accuracy of $\approx \pm 200$ mV. Fluctuations of the order of ± 300 mV around the time-averaged value of 2498.0 V were observed. Hence, it is believed that the Ps^- acceleration voltage U_{Ps^-} is known to be better than ± 1 V, which leads to a relative error of 0.2‰ in Γ. For the initial energy of the Ps^- ions of $T_0 = 0.3$ eV, an error of 100% is assumed, which results in an additional uncertainty of Γ of 0.07‰.

The displacement of the accelerated positron beam on the DLC foil when changing the decay gap width between 3.1 and 21.1 mm could be limited to <0.2 mm (see Sec. III B). Nevertheless, depending on the size and morphology of the inhomogeneities of the foil, this might lead to changes in the Ps^- production probability. While even a hole in the foil of the area of a basic mesh square (0.006 mm^2), which we would have easily spotted during the microscope inspection, would only contribute at most 0.15‰ to the error budget of Γ, effects of foil inhomogeneities may be considerably larger. Unfortunately, only little is known about the homogeneity of DLC foils, but nonuniformities of up to $\pm 25\%$ have been claimed [35]. Because the spacial structure of these reported inhomogeneities are likely much smaller than the size of the e^+ beam, they would average out for any displacement of the beam. Smooth variations of the average thickness of the foil are of more concern. Assuming, for example, a smooth Gaussian-like change of the foil thickness by 20% over the foil radius of 6 mm, average changes of the Ps^- production probability of about 0.5‰ are found to occur for beam shifts of 0.2 mm, depending on the position of the center of the Gaussian with respect to the e^+ beam. However, for some shift directions, deviations of up to 0.9‰ may occur; we will use this number as a conservative estimate of the contribution of foil inhomogeneities to the systematic error budget of Γ.

TABLE I. Systematic error contributions to the present measurement of the Ps^- decay rate Γ.

Error source	Absolute (ns^{-1})	Relative (‰)
U_{Ps^-}	0.0004	0.2
T_0	0.0002	0.1
Ps^- production	0.0019	0.9
Positron flux	0.0003	0.2
Positioning	0.0011	0.5
Timing	0.0000	0.0
Total	0.0023	1.1

As discussed in Sec. III B, the positron flux decreased by about 1‰ per measurement cycle. Since in each of the 50 cycles in the production run the order at which the different gap widths were measured was randomly changed, the systematic error due to the assumption of a constant flux can be conservatively estimated to be less than $1/\sqrt{50}$‰ = 0.15‰.

Based on the specifications given by the manufacturer of the linear translation table for the position reproducibility and the angular errors, the overall uncertainty in the decay gap width determination is estimated to be 3 μm [21]. This uncertainty has been accounted for by calculating the count rate change connected with a distance change of 3 μm and considering it as an additional systematic error in the Ps^- count rate. This leads to a systematic error contribution to Γ of 0.51‰.

The dead time of the data acquisition system was around 1.2‰ at all distances. The dead time was automatically taken care of by using the system lifetime to control the timing. No systematic error contribution to Γ is expected from this source (<0.01‰).

The estimated systematic errors are compiled in Table I. They are dominated by our limited knowledge of the DLC-foil inhomogeneities. By adding these errors up quadratically, the total systematic uncertainty of the Ps^- decay rate is estimated to be ± 0.0023 ns^{-1} (1.1‰), a factor of 2 smaller than the statistical error of ± 0.0044 ns^{-1} (2.1‰). Combining both errors, one finally obtains for the Ps^- decay rate

$$\Gamma = 2.0875(50)\,ns^{-1}.$$

V. SUMMARY AND CONCLUSION

Compared to the Ps^- decay rate of $\Gamma = 2.089(15)\,ns^{-1}$ obtained in the previous experiment [22], a precision three times more accurate (2.4‰) could be reached in the present study. This improvement is due to the advanced control of potential sources of systematic errors that could be achieved by upgrading the setup and due to improved statistics, which was

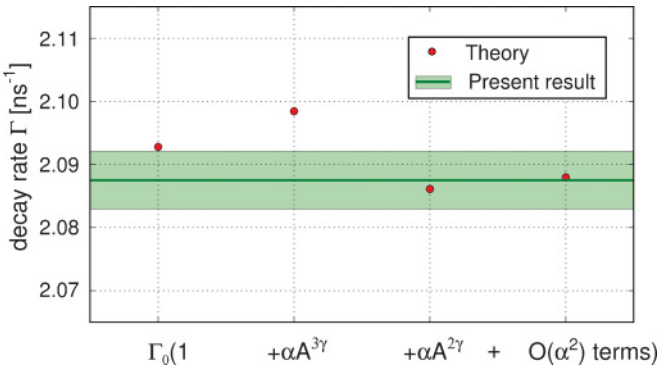

FIG. 10. (Color online) Calculated Ps^- decay rate according to [5] in comparison to the measured value from the present work. The (red) dots are reflecting the running sum over the lowest terms in the expansion of Γ in terms of the fine-structure constant α.

made possible by the larger flux (by 100 times) of moderated positron available at the NEPOMUC positron source.

The present result is in very good agreement with the most recent theoretical value of $\Gamma = 2.087\,963(12)\,\mathrm{ns}^{-1}$ [5], which contains now all correction terms up to order $O(\alpha^2)$. In Fig. 10, the running sum over the correction terms to Γ, the $O(\alpha)$ terms $A^{3\gamma}$ from the zero-order contribution of the 3γ decay and $A^{2\gamma}$ denoting the first-order radiative correction term to the 2γ decay, and the $O(\alpha^2)$ terms are shown and compared to the present experimental value (see also Sec. II). While it is obvious that due to the recent work of Puchalski *et al.* theory is again far ahead of experiment, with the present experimental precision we are now able to probe theoretical calculations of the decay rate to the precision of the leading-order QED corrections $A^{3\gamma}$ and $A^{2\gamma}$. As these terms are also probed by the ortho- and para-positronium decay rates, respectively, we may use this knowledge to determine from the measured Ps^- decay rate the genuine three-body quantity $\langle\delta_{+-}\rangle$, which describes the probability of finding the annihilating electron-positron pair at the same position. This results in

$$\langle\delta_{+-}\rangle = 0.020\,729(50), \tag{17}$$

which is to be compared with the theoretical value of $\langle\delta_{+-}\rangle = 0.020733\ldots$ believed to be known up to an accuracy of 10^{-11} [5].

While there may be room for a further increase of the statistical accuracy of the Ps^- decay rate Γ, a decisive improvement of the experimental precision likely requires an alternative measurement technique. Our present experimental efforts are concentrated on the measurement of the Ps^- photodetachment cross section and the production of a monoenergetic ortho-positronium beam.

ACKNOWLEDGMENTS

We thank V. K. Liechtenstein for providing us with the thin DLC foils. This project was partly funded by DFG under HA1101/13-1. D.S. acknowledges support by the Weizmann Institute for Science through the Joseph Meyerhoff program.

[1] J. Wheeler, Ann. NY Acad. Sci. **47**, 219 (1946).
[2] H. A. Bethe and E. E. Salpeter, *Quantum Mechanics of One- and Two-Electron Atoms* (Springer-Verlag, New York, 1957).
[3] V. I. Korobov, Phys. Rev. A **61**, 064503 (2000).
[4] A. M. Frolov, Phys. Lett. A **342**, 430 (2005).
[5] M. Puchalski, A. Czarnecki, and S. G. Karshenboim, Phys. Rev. Lett. **99**, 203401 (2007).
[6] E. A. Hylleraas, Phys. Rev. **71**, 491 (1946).
[7] M. Barham and J. W. Darewych, J. Phys. B **41**, 185001 (2008).
[8] G. W. F. Drake and M. Grigorescu, J. Phys. B **38**, 3377 (2005).
[9] G. W. F. Drake, M. M. Cassar, and R. A. Nistor, Phys. Rev. A **65**, 054501 (2002).
[10] A. Bhatia and R. J. Drachman, Nucl. Instrum. Methods Phys. Res. B **143**, 195 (1998).
[11] A. M. Frolov, Phys. Rev. A **60**, 2834 (1999).
[12] Y. K. Ho, Phys. Rev. A **48**, 4780 (1993).
[13] A. K. Bhatia and R. J. Drachman, Phys. Rev. A **32**, 3745 (1985).
[14] S. J. Ward, J. W. Humberston, and M. R. C. McDowell, J. Phys. B **20**, 127 (1987).
[15] V. B. Mandelzweig, Nucl. Phys. A **508**, 63C (1990).
[16] C. D. Wensheng Bian, Int. J. Quantum Chem. **51**, 285 (1993).
[17] R. Krivec, V. B. Mandelzweig, and K. Varga, Phys. Rev. A **61**, 062503 (2000).
[18] A. P. Mills, Phys. Rev. Lett. **46**, 717 (1981).
[19] A. P. Mills, Phys. Rev. Lett. **50**, 671 (1983).
[20] D. Schwalm, F. Fleischer, M. Lestinsky, K. Degreif, G. Gwinner, V. Liechtenstein, F. Plenge, and H. Scheit, Nucl. Instrum. Methods Phys. Res. B **221**, 185 (2004).
[21] F. Fleischer, Ph.D. thesis, Max Planck Institut für Kernphysik Heidelberg, 2005, http://www.ub.uni-heidelberg.de/archiv/5588.
[22] S. M. Fleischer, K. Degreif, G. Gwinner, M. Lestinsky, V. Liechtenstein, F. Plenge, and D. Schwalm, Phys. Rev. Lett. **96**, 063401 (2006).
[23] K. Michishio, T. Tachibana, H. Terabe, A. Igarashi, K. Wada, T. Kuga, A. Yagishita, T. Hyodo, and Y. Nagashima, Phys. Rev. Lett. **106**, 153401 (2011).
[24] C. Hugenschmidt, K. Schreckenbach, M. Stadlbauer, and B. Straßer, Nucl. Instrum. Methods Phys. Res. B **554**, 384 (2005).
[25] A. M. Frolov, e-print arXiv:0905.2454.
[26] S. I. Kryuchkov, J. Phys. B **27**, L61 (1994).
[27] S. G. Karshenboim, Int. J. Mod. Phys. A **19**, 3879 (2004).
[28] C. Hugenschmidt, B. Löwe, J. Mayer, C. Piochacz, P. Pikart, R. Repper, M. Stadlbauer, and K. Schreckenbach, Nucl. Instrum. Methods Phys. Res. A **593**, 616 (2008).
[29] C. Piochacz, G. Kögel, W. Egger, C. Hugenschmidt, J. Mayer, K. Schreckenbach, P. Sperr, M. Stadlbauer, and G. Dollinger, Appl. Surf. Sci. **255**, 98 (2008).
[30] V. K. Liechtenstein, T. M. Ivkova, E. D. Olshanski, I. Feigenbaum, R. DiNardo, and M. Döbeli, Nucl. Instrum. Methods Phys. Res. A **397**, 140 (1997).

[31] J. Levin, L. Knoll, M. Scheffel, D. Schwalm, R. Wester, A. Wolf, A. Baer, Z. Vager, D. Zajfman, and V. Liechtenstein, Nucl. Instrum. Methods Phys. Res. B **168**, 268 (2000).

[32] H. Ceeh, Master's thesis, Technische Universität München, 2009.

[33] H. Ceeh, S. Gärtner, C. Hugenschmidt, K. Schreckenbach, D. Schwalm, and P. Thirolf, J. Phys.: Conf. Ser. **262**, 012011 (2011).

[34] F. James and M. Roos, Comput. Phys. Commun. **10**, 343 (1975).

[35] K. McDonald, R. A. Weller, and V. Kh. Liechtenstein, Nucl. Instrum. Methods Phys. Res. B **152**, 171 (1999).